New sampling device for on-site measurement of SVOC gas-phase concentration at the emitting material surface

Mylène Ghislain, J. Beigbeder, H. Plaisance, V. Desauziers

New sampling device for on-site measurement of SVOC gas-phase concentration at the emitting material surface

Mylène Ghislain[1] · **Joana Beigbeder**[1] · **Hervé Plaisance**[1] · **Valérie Desauziers**[1]

Abstract The gas-phase concentration at the material surface (y_0) is pointed out in the literature as a key parameter to describe semivolatile organic compound (SVOC) emissions from materials. This is an important input data in predictive models of SVOC behavior indoors and risk exposure assessment. However, most of the existing measurement methods consist of determining emission rates and not y_0 and none allow on-site sampling. Hence, a new passive sampler was developed. It consists of a glass cell that is simply placed on the material surface until reaching equilibrium between material and air; y_0 is then determined by solid-phase microextraction (SPME) sampling and GC-MS analysis. The limits of detection are at the μg/m^3 level and relative standard deviations (RSD) below 10%. A variation of 11% between two sets of experiments involving different cell volumes confirmed the y_0 measurement. In addition, due to the ability of SVOCs to be sorbed on surfaces, the cell wall/air partition was assessed by determining the inner cell surface concentration of SVOCs, which is the concentration of SVOCs adsorbed on the glass, and the cell surface/air partition coefficient (K_{glass}). The recovery yields of the SVOCs sorbed on the cell walls are strongly compound-dependent and comprise between 2 and 93%. The K_{glass} coefficients are found to be lower than the stainless steel/air partition coefficient (K_{ss}), showing that glass is suitable for the SVOC sampling. This innovative tool opens up promising perspectives in terms of identification of SVOC sources and quantification of their emissions indoors, and would significantly contribute to human exposure assessment.

✉ Valérie Desauziers
valerie.desauziers@mines-ales.fr

[1] C2MA, Ecole des Mines d'Alès, Hélioparc, 2 Avenue Pierre Angot, 64053 Pau Cedex 9, France

Keywords Material/air interface concentration (y_0) · SVOCs · Emission cell · Indoor air · Organophosphate esters · Flame retardants

Introduction

Semivolatile organic compounds (SVOCs), such as flame retardants, plasticizers, or preservatives, are present in many building materials and household products. Their incorporation rates in these products are significant: SVOCs typically constitute 1–30% of the material composition [1, 2]. According to their physicochemical properties and incorporation modes, they are subject to diffusion and migration within the material and then can be emitted to the surrounding air. Owing to their wide use, the growing occurrence of SVOCs in indoor environments, including air [1, 3–5] and dust [6–10], have been reported. The indoor concentrations were found to be much higher than outdoor ones [11], showing the contribution of indoor emitting sources such as materials. Because of their properties, emitted SVOCs are divided between gas phase, suspended particles, settled dust, and surfaces (including furniture, human skin, or clothing) [2, 12–14], leading to numerous exposure pathways: inhalation, ingestion, especially for young children with hands–mouth contact, and skin contact. Some of SVOCs are suspected to be carcinogenic [15–17], neurotoxic [18], or endocrine disruptors [19, 20]. Because of these suspected adverse health effects and their ubiquitous presence indoors, it is necessary to understand, even more to predict, the SVOCs partitioning between the different compartments of indoor environments. In this aim, the identification and characterization of the material sources are challenging issues.

In literature, few methods describe the measurement of SVOCs emissions from materials. Different parameters can

be determined to characterize emissions: the emission rate or the gas-phase concentration at the material surface (y_0). This concentration is a key parameter for material emission characterization, indoor air quality modeling [21], and risk exposure assessment [22]. However, conventional methods generally determine emission rates under laboratory conditions [23–28]. The compounds emitted by the material in the gas volume of a chamber (or cell) are recovered by pumping through a filter or an adsorbent tube (Tenax) connected to the outlet of the chamber. However, a commonly reported issue for these methods is the loss of SVOCs due to sink effects (adsorption on the sampler walls) which tends to underestimate emissions [2, 14, 29]. Because of their low vapor pressure, SVOCs are partially sorbed on the large inner surfaces of these chambers at ambient temperature (23 °C), affecting the results [23]. This is why the ISO 16000-25 standard relative to the determination of the emission of SVOCs by building products in micro-chamber includes a high temperature (220 °C) desorption step for a total recovery of the emitted compounds [30]. On the same principle, Katsumata et al. [29] conducted sampling in two steps: after removal of the test material, the chamber is heated to 250 °C to collect the fraction of SVOCs adsorbed on the inner walls. Another efficient way is to reduce the sink effects by minimizing the ratio of the internal chamber surfaces over the emission surface area [23]. For that, a sandwich-like chamber was especially designed, thus limiting sorption of SVOCs onto inner sampler walls [31–33]. Recently, this sandwich-like chamber was adapted by Cao et al. [34] to determine the gas-phase concentration at the material surface (y_0) instead of the emission rate. In the new configuration, the chamber is fully closed, without airflow. Under these conditions, the mass transfer is governed by the diffusion of compounds from the tested material to the chamber air. The compounds are emitted by the material until reaching equilibrium between the material and chamber air. From first Fick law under steady state conditions [35], the concentration in the chamber can be assimilated to the concentration y_0, which is measured by introducing a solid-phase microextraction (SPME) fiber into the chamber via a septum (this approach is similar to that we developed for VOCs, which is described in the following [36]). However, these different methods of emission measurement are performed in the laboratory and thus are not representative of real indoor environments: they neither consider the conditions of implementation of materials nor the possible effects of assemblies on emission (e.g., for furniture, the layering of cushioning foam, interlining materials, and coatings). In the aim of on-site determining y_0, a simple method using standard stainless steel thermal desorption tube as passive sampler has been recently developed [37]. The compactness and the low cost of this tube allow multiplying easily the sampling points. After sampling, the total SVOCs amount inside the tube is thermally desorbed and analyzed. The sorbed part on inner surface of tube is included in the quantified amount. Therefore, the gas-phase SVOCs concentration at the material surface cannot be directly measured but is deduced from modeling of the sorbed part. Another approach is to assume that y_0 could be considered equal to the vapor pressure of the pure SVOCs [26, 31]. As this assumption is only valid for high weight percentages of SVOCs in consumer products, it cannot be generalized [38, 39] and y_0 is not directly available for many SVOCs. Therefore, the development of an on-site method to determine the gas-phase SVOCs concentration at the material surface is relevant and constitutes the main objective of this work. The considered device is inspired by a system previously developed in our laboratory for on-site measurement of y_0 for VOCs [36]. It consists of coupling a home-made glass cell (DOSEC) with SPME. The DOSEC is placed directly on the material surface. First, compounds diffuse from the material surface to the headspace of the cell until reaching equilibrium [35, 38], and secondly, y_0 is determined by passive SPME sampling and gas chromatography analysis (contrary to SVOCs, the sorbed part on inner surface of cell is negligible for VOCs).

The aim of this study was to determine experimentally the SVOCs gas-phase concentration (y_0) at the emitting material surface. For this, the DOSEC geometry was adapted to limit SVOCs losses by sink effects and to shorten the time to reach material/air equilibrium. The feasibility of this method was studied on organophosphate esters (OPs), which are widely used [40], mainly as polybrominated diphenyl ethers (PBDE) flame retardant substitutes [8, 41–44]. After the validation of the principle of y_0 measurement, the performance of the method as limits of detection and reproducibility were determined. The cell was also designed to recover the fraction sorbed on its inner surface (q_s) during a sampling step involving vacuum/heating cycles. The cell surface/air partition coefficient (K_{glass}) was thus assessed and compared with data available in the literature for other SVOCs and sampler materials (e.g., stainless steel).

Materials and methods

Material samples and target SVOCs

This study was conducted on materials synthetized in the laboratory: two soft polyurethane foams (PU) containing seven organophosphate esters (Table **1**) with individual concentrations of 5 and 7.6 wt% , respectively, were implemented [46]: TBP, TCEP, and TCP (isomers mixture) standards were supplied by Sigma-Aldrich (St. Louis, MO, USA), TEP by Merck (Darmstadt, Germany), TPP, TCPP (isomers mixture), and TDCPP by ICL-products (Amsterdam, The Netherlands). These compounds were selected to evaluate the method over a wide range of physicochemical properties (volatility,

Table 1 Physicochemical properties of target SVOCs (estimated values [45]) and ions for SIM acquisition (*m/z*)

		Formula	CAS	Boiling point (°C)	Vapor pressure (Pa) at 25 °C	Log K_{oa} at 25 °C	Ion for SIM acquisition (m/z)
TEP	Triethyl phosphate	$(C_2H_5O)_3PO$	78-40-0	233	2.20×10^{1}	6.632	99
TBP	Tributyl phosphate	$(CH_3(CH_2)_3O)_3PO$	126-73-8	327	4.65×10^{-1}	8.239	99
TCEP	Tris(2-chloroethyl)-phosphate	$(ClCH_2CH_2O)_3P(O)$	115-96-8	352	5.21×10^{-2}	5.311	63
TCPP	Tris-(chloropropyl)-phosphate	$C_9H_{18}Cl_3O_4P$	13674-84-5	365	7.52×10^{-3}	8.203	99
TCP	Tricresyl phosphate	$(CH_3C_6H_4O)_3PO$	1330-78-5	476	8.00×10^{-5}	9.591	99
TPP	Triphenyl phosphate	$(C_6H_5O)_3PO$	115-86-6	441	6.29×10^{-5}	8.459	326
TDCPP	Tris-(dichloropropyl)-phosphate	$C_9H_{15}Cl_6O_4P$	13674-87-8	459	3.81×10^{-5}	10.622	368

K_{oa}: octanol/air partition coefficient.

octanol/air partition coefficient). The amounts of organophosphate esters incorporated and the manufacturing process are typical for foams used in the furniture sector. Polyurethane foams were cut into 41 × 24 cm panels with a thickness of 1 cm and a density of 200 kg/m^3. Samples were stored in aluminum foil at room temperature [47] and conditioned in an environmental chamber under a humid airflow (50% RH) for 24 h before sampling.

Sampling device

The developed sampler was a 60 mL glass emission cell with a cylindrical shape and a sampling area of 17 cm^2 (Fig. 1). Glass (borosilicate 3.3) was chosen because it is an inert material easy to implement and inexpensive. The top of the cell has a cap with a septum for SPME fiber introduction. The bottom is fitted with a thread for hermetically sealing the cell with a silonite-coated stainless steel screw cap equipped with a high-vacuum valve. The sealed cell supports a vacuum of 50 mmHg at high temperature (typically 100 °C). For the needs related to the development of the method, another cell of 120 mL was manufactured. The design of this cell is identical to the previous one, with the same sampling surface, but its volume is twice as high.

Sampling cells were cleaned before and after each use with methanol rinsing (≥99%, Sigma-Aldrich, St Louis, MO, USA). After drying, some vacuum/clean air filling cycles complemented the procedure.

y_0 Measurement

During the first sampling step, the cell was placed directly on the material for a defined time during which OPs was emitted inside the gas volume of the cell. When material/air equilibrium was reached, a SPME fiber was introduced in the cell for passive sampling of SVOCs in the gas phase (Fig. 1). A 100 μm polydimethylsiloxane (PDMS) fiber was selected (Supelco, Bellefonte, PA, USA) according to the studies showing that this coating is suitable for organophosphate esters extraction [48–51]. After preliminary tests, an extraction time of 15 min was selected, corresponding to a good compromise between sensitivity and analysis time. The

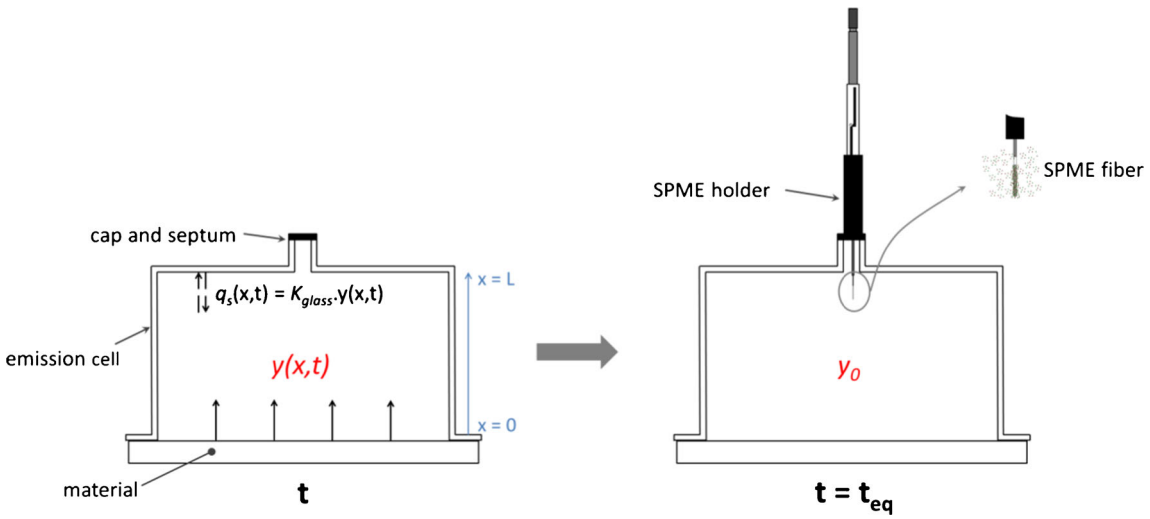

Fig. 1 Sampling of gas-phase SVOCs concentration at emitting material surface. *y*: gas-phase concentration in the cell headspace. y_0: gas-phase concentration at the material surface. q_s: cell surface concentration. K_{glass}: cell surface/air partition coefficient

temperature was controlled and maintained at 23 °C during these tests. Preliminary tests demonstrated that the SPME fiber did not disturb the equilibrium within the cell: the analysis of seven successive extractions in the same cell headspace showed a variation less than 5%.

After sampling, the SPME fiber was directly desorbed in the injector port of a gas chromatograph for analysis. A Varian CP-3800 gas chromatograph coupled to a 1200Q quadrupole mass spectrometer (MS) (Varian, Les Ulis, France) was used. The PTV 1079 injection port was equipped with a 0.75 mm i.d. liner and operated at 250 °C in splitless mode. The carrier gas was helium with a flow rate of 2 mL/min. A 5% phenyl capillary column of 60 m, 0.25 mm i.d., and a 1 μm film thickness was used. The oven temperature was maintained at 60 °C for 2 min, then ramped at 30 °C/min to 200 °C, held for 2 min, then ramped at 15 °C/min to 310 °C, held for 22 min. The transfer line to the MS and the ion source were maintained at 250 °C. Single ion monitoring (SIM) acquisition was carried out at 0.4 scan/s in electron impact mode (70 eV): the selected ions are presented in Table 1. The identification was confirmed by retention times of commercial standards.

An external calibration method was specifically developed and applied for the quantification of target analytes by SPME method: test atmospheres were generated by vaporization of OPs methanolic solutions in the cell at reduced pressure (50 mmHg). The cell was then filled with clean air (Zero air generator AZ2020R; Claind, Lenno, CO, Italy). Calibration was based on the relationship found between the quantification by the active sampling method using Tenax tubes and the SPME method. The SPME procedure was identical to the sample ones. The sampling with Tenax tubes was intended to quantify the gaseous fraction of OPs in the cell previously loaded with standard solutions. The cell was flushed at room temperature and atmospheric pressure with clean air with a low flow rate of 60 mL/min for 5 min to collect only the gaseous fraction of OPs on Tenax tubes at the cell output. Tenax cartridges were then thermodesorbed and analyzed under the same conditions as those used for the sorbed fraction analysis (described in the following section). Calibration curves were established with a minimum of five concentration levels in the range as those obtained for the samples (0.05–500 mg/m^3).

Surface sorption measurement

A fraction of the emitted compounds is sorbed to the inner cell surface [2, 14, 29, 37]. It is assumed that the partition between air and the inner cell surface follows a linear sorption isotherm [37, 38]. This assumption is only true for initial period (i.e., low y_0 values) but likely not so as system approaches saturation. Thus,

$$q_s = K_{glass}.y_0 \quad (1)$$

where q_s (μg/m^2) is the concentration of SVOCs sorbed at the cell surface, y_0 (μg/m^3) is the gas-phase concentration at the emitting material surface, and K_{glass} (m) is the cell surface/air partition coefficient.

To recover the SVOCs sorbed onto the inner walls of the sampler, a second sampling step, which did not involve the emitting surface, was performed. Knowing the total inner surface area of the cell, the sorbed surface concentration (q_s) can be determined. After closing with the screwcap, the cell was placed in an oven. Since different elements of the cell (seals, septum…) did not allow a high temperature heating, several heating cycles at 100 °C combined with vacuum pumping (up to 50 mmHg) were carried out (Fig. 2). This combination of temperature/pressure was chosen to achieve the vaporization conditions of TCPP (vapor pressure = 40 mmHg at 110 °C). The sorbed fraction was collected in a stainless tube containing 250 mg of Tenax TA supplied by PerkinElmer (Waltham, MA, USA) and analyzed by automated thermal desorption

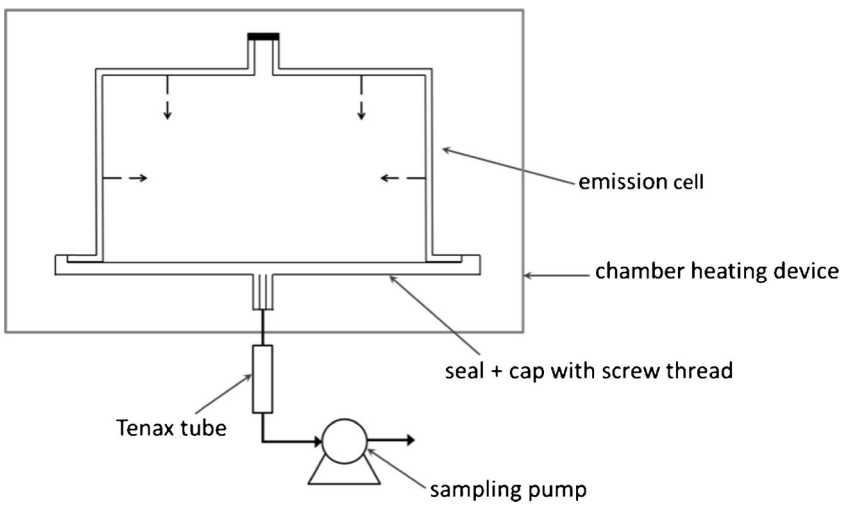

Fig. 2 Recovery of sorbed SVOCs

(ATD) coupled to GC-MS. Sampling tubes were cleaned before and after each use with pure helium gas at a flow rate of 100 mL/min at 320 °C for 15 min. Quantification of OPs was made with an external calibration. For this, Tenax tubes were loaded with 1 μL of standard mixtures with a conventional GC syringe and purged for 5 min with pure helium at flow rate of 50 mL/min to evaporate the solvent.

To determine the recovery yields, known amounts (16–100 ng) of standard mixtures were introduced in the closed cell with a syringe. The recovery procedure was then applied and OPs were collected into Tenax tubes. In parallel, the same amounts of OPs were directly loaded into Tenax tubes to serve as references. The ratio between the result obtained with the addition of standard solutions into the cell and that obtained with the direct loading of these same standard solutions in the tube corresponds to the recovery rate.

Analysis was carried out with a PerkinElmer TurboMatrix 650 ATD thermal desorption system (Waltham, MA, USA). The Tenax tubes were heated at 320 °C for 15 min, using a helium flow rate of 100 mL/min without inlet split to desorb the analytes and focus them into an air monitoring cold trap kept at 0 °C. Desorption trap was ramped at 99 °C/min to 350 °C, held for 10 min, with an outlet split of 5 mL/min. The transfer line to the GC and the valve were maintained at 250 °C. Separation and detection were performed with a PerkinElmer Clarus 680 gas chromatograph. The carrier gas was helium with a flow rate of 1.3 mL/min. A 5% phenyl capillary column of 60 m, 0.25 mm i.d. and a 0.25 μm film thickness was used. The oven temperature was maintained 2 min at 50 °C, then ramped at 15 °C/min to 200 °C, held for 2 min, then ramped at 15 °C/min to 300 °C, held for 14 min. The gas chromatograph was equipped with a PerkinElmer Clarus SQ 8 T mass spectrometer (MS). The transfer line to the MS and the ion source were maintained at 180 °C. Acquisition was carried out in single ion monitoring (SIM) in electron impact mode (70 eV): the selected ions are presented in Table 1. Analytical conditions (inlet and outlet split, flow rates, temperatures, etc.) were chosen on the basis of previous works [52].

Analytical system blanks

To check the contamination level and memory effect due to the analytical systems, analytical blanks and sampling blanks (analysis of empty closed cells) were performed. No contamination due to cells, SPME fibers, Tenax tubes, analytical systems, laboratory air, and clean air was observed in the selected analytical conditions. Furthermore, blanks during the ATD sequences proved that there was no memory effect between two consecutive analyzed samples.

Results and discussions

Measurement of the gas-phase concentration at the material surface (y_0)

For determining the material/air equilibrium time required for y_0 measurement, OPs emission kinetics were studied at 23 °C using the PU + 7.6% OPs foam. The cell was placed on the material surface for increasing periods. After each period, a 15 min SPME sampling was performed to determine the concentration of OPs in the gas phase. The results are shown in Fig. 3a. After SPME extraction, the cell was hermetically closed with the screw cap and the OPs fraction sorbed on the inner walls of the cell was recovered on a Tenax tube by applying the heating/pumping procedure described above.

Only TEP, TBP, and TCPP could be quantified in the gas phase. TCEP was detected but its quantification was limited because of the too low standard concentration generated in the cell for calibration. TDCPP, TPP, and TCP were not detected either in the gas-phase or on sampler surface. Figure 3a shows that emission kinetic depends on volatility: equilibrium is reached very quickly for TEP (after 30 min), whereas 2 h is needed for TBP. Globally, for the OPs detected in the gas phase, equilibrium is reached after 3.5 h.

The sorbed surface concentrations of organophosphate esters increase progressively until reaching equilibrium with air in the cell. Sorption kinetic depends on the compounds and their volatility: as emission kinetic, the most volatile compound has the faster sorption kinetic. The time to reach equilibrium is from 3 to 5 h (Fig. 3b). Thus, sorption kinetic is slower than kinetic relative to gas-phase concentration. This result was expected since the sorption kinetics depend on intake of SVOCs by emission. Indeed, whereas the initial emission rate (deduced from the initial slope of gas-phase concentration increasing) for TEP is about 8000 ng/h, the sorption rate is only 70 ng/h. This difference is lower for the less volatile compounds: for TCPP, the initial emission rate is about 14 ng/h and the initial sorption rate is 4.5 ng/h. These results provide first information about the behavior of the compounds in the cell and their partition between the two phases; this information will be complemented with y_0 and surface sorption measurements.

As the sorption on the inner walls of the cell is the limiting parameter, all measurements of y_0 and q_s were performed after an equilibrium time of 5 h. In these conditions, both material/air and air/surface equilibria are reached. This sampling time is quite acceptable for on-site measurements.

Validation of y_0 measurement

To be sure of really measuring y_0, the 60 mL cell was compared with a 120 mL one. Obviously, the increase in volume for the same sampled surface induces an increase in the ratio

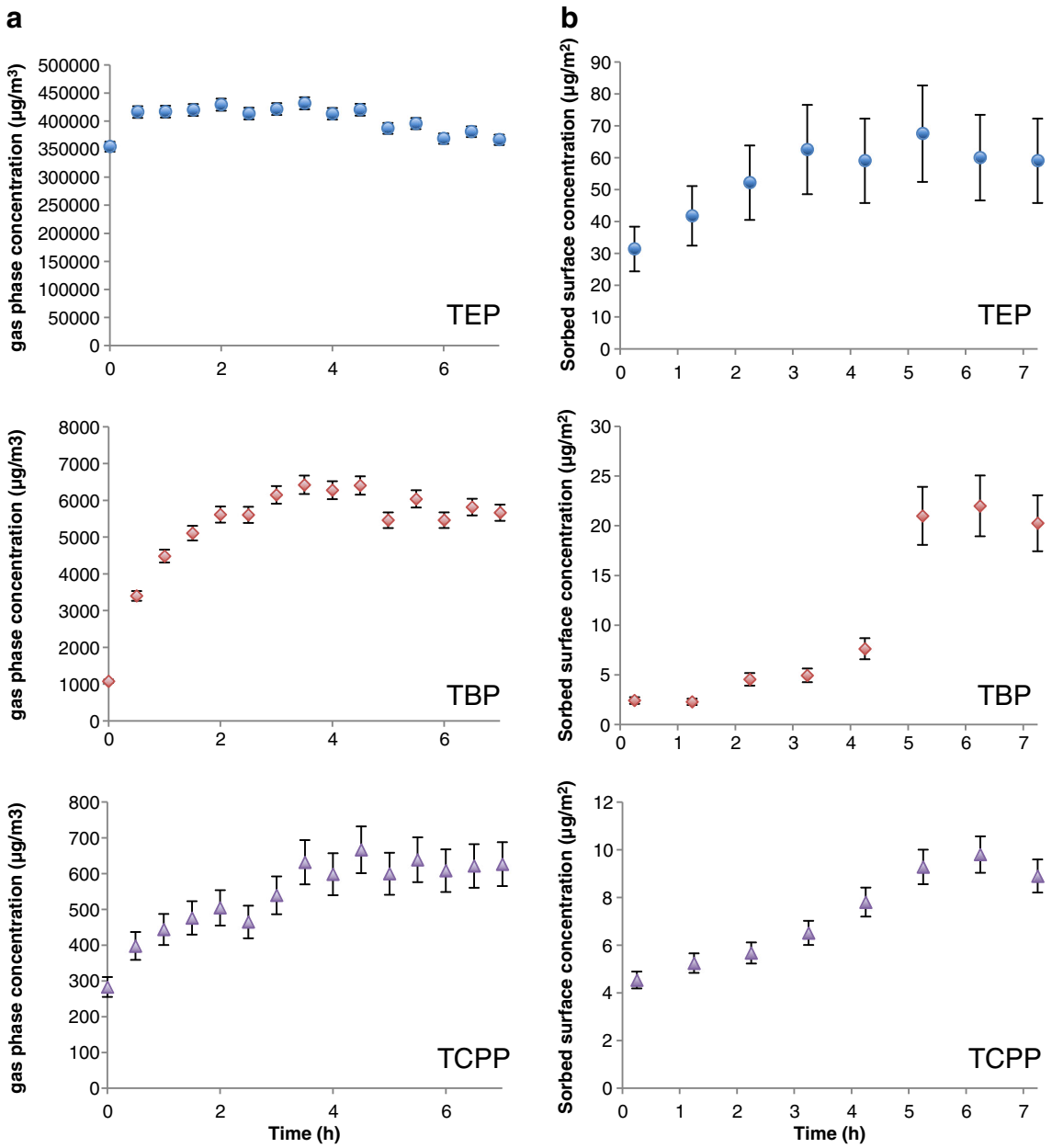

Fig. 3 Time variation in gas-phase cell concentration of organophosphate esters emitted from soft polyurethane foam (**a**). Time variation in sorbed amounts of organophosphate esters on cell inner surface (**b**). TCEP, TCP, TPP, and TDCPP: not quantifiable

sorption surface/emission surface, with a sorption surface 1.75 times larger for the 120 mL cell.

According to the Student *t*-test, there is no significant difference in the gas-phase concentration at equilibrium between the 60 mL and the 120 mL cells, at a confidence level of 95% (Table 2). Increasing the sorption surface (i.e., increasing the cell volume) leads to increase equilibrium time between material (PU foam) and air (up to six times longer than for the 60 mL sampler) but does not change the gas-phase concentration at equilibrium. It shows that the sampler geometry itself does not influence the measurement and that the gas-phase concentration y in the cell headspace at equilibrium corresponds to the gas-phase concentration at the material surface y_0, thereby validating the principle of y_0 measurement.

The standard deviations determined from five replicates show a low variability (<15%) of the y_0 measurement in the 60 mL cell; therefore, a homogeneous gas-phase concentration can be stated in the whole cell gas volume. Because of the height of the cells, the SPME fiber could not be placed at the same distance from the surface of the material in the two different cells. However, the measured concentrations are not significantly different, thus assuming that there is no concentration gradient within the cells.

Table 2 Measured values of y_0, at 23 °C (mg/m^3) and comparison of the two cells (PU + 7.6% OPs material). Standard deviations are calculated from five replicates

	60 mL cell		120 mL cell	Comparison of the two cells	
	PU + 5% OPs	PU + 7.6% OPs	PU + 7.6% OPs	% Difference	*p*-value (*t*-test)
TEP	198 ± 4	380 ± 12	336 ± 64	11.6	0.17
TBP	1.46 ± 0.05	5.7 ± 0.3	5.1 ± 1.2	10.5	0.28
TCPP	0.27 ± 0.04	0.63 ± 0.03	0.58 ± 0.17	7.9	0.51

For a same initial amount of OPs incorporated into the foam, y_0 values are very different depending on the volatility of compounds (Table 2): the more volatile the compound, the higher the gas-phase concentration. This concentration tends to increase with the content of organophosphate esters in polyurethane foams, but not proportionally. Despite the realistic incorporation rates and mode (additive process) [8], the emitted amounts are very high (y_0 in the mg/m^3 order level), showing a strong ability of the polyurethane foams to release OPs. This confirms the results of a previous study [46], where OPs were detected at high levels in commercial cushioning foams manufactured by additive process. This shows the important impact that upholstered furniture may have as flame retardant sources indoors.

Recovery of SVOCs sorbed on the inner cell walls

Three amounts of the target compounds were spiked in the cell (16, 50, and 100 ng) and for each, several heating/pumping cycles were applied (6, 7, and 8 cycles). Results summarized in Table 3 show that the amount spiked in the cell has no influence on the recovery efficiency. Combining heating with a controlled vacuum seems also to be effective for desorption of OPs of different volatilities: the most volatile (TEP) and the least volatile (TDCPP) are quantitatively recovered after six heating/pumping cycles (83 and 103%, respectively). However, the recovery rates tend to decrease when the number of cycles increases. TBP, TCEP, and TCPP recoveries are improved for seven heating/pumping cycles: 53, 18, and 93%, respectively, whereas TPP and TCP are poorly recovered regardless the number of cycles. The breakthrough of the Tenax tube may explain losses when the number of cycles increases due to the high temperature and low pressure conditions applied. Using two Tenax tubes in series was tested but did not improve the recovery: under these conditions, the pressure drop is too important to reach an adequate vacuum in the cell. Furthermore, since adsorption is an exothermic phenomenon, the temperature and pressure conditions selected to desorb OPs from the cell walls are obviously unfavorable for adsorption on Tenax.

Finally, the best compromise for the largest number of compounds is seven cycles, regardless of the amount spiked in the cell. This method allows the quantitative recovery of TCPP and TDCPP sorbed onto the inner cell surfaces with upper recovery rates to 80%: 93 ± 17 and 89 ± 17%, respectively. With upper recovery rates to 60%, TEP (70 ± 18%) and TBP (63 ± 20%) can also be quantified by taking the recovery yields into account in the calculation.

Measurement of the sorbed surface concentration (q_s)

As for the gas phase, only TEP, TBP, and TCPP were detected on inner sampler walls, and the sorbed surface concentration (q_s) was also shown to be compound-dependent (Table 4). For the most volatile SVOCs (e.g., TEP), q_s values are higher than for the least volatile compounds due to a higher initial

Table 3 Average ± standard deviation of recovery rates (%) of OPs sorbed onto the inner cell surface for different spiked amounts (*n = number of replicates*). In bold: recovery yields above 60%

Amount spiked in the cell	16 ng (n = 1)			50 ng (n = 5)			100 ng (n = 7)		
Heating/pumping cycles number	6	7	8	6	7	8	6	7	8
TEP	**89**	**74**	20	**78 ± 31**	**68 ± 16**	15 ± 11	**81 ± 33**	**68 ± 19**	12 ± 8
TBP	31	**60**	9	40 ± 8	**72 ± 21**	12 ± 3	32 ± 8	56 ± 19	8 ± 1
TCEP	12	16	6	18 ± 8	18 ± 18	8 ± 4	16 ± 8	20 ± 23	10 ± 4
TCPP	45	**98**	25	24 ± 4	**89 ± 11**	8 ± 1	20 ± 4	**93 ± 22**	10 ± 1
TCP	2	8	3	1 ± 1	9 ± 9	5 ± 5	3 ± 3	11 ± 10	6 ± 7
TPP	2	3	0	4 ± 2	2 ± 2	0	3 ± 1	3 ± 3	1 ± 3
TDCPP	**99**	**91**	20	**102 ± 13**	**88 ± 13**	14 ± 13	**107 ± 19**	**89 ± 20**	40 ± 32

Table 4 Measured values q_s, at 23 °C (μg/m^2) and comparison of the two cells (PU + 7.6% OPs material). Standard deviations are calculated from five replicates

	60 mL cell		120 mL cell	Comparison of the two cells
	PU + 5% OPs	PU + 7.6% OPs	PU + 7.6% OPs	% Difference
TEP	39 ± 8	62 ± 15	62 ± 12	0
TBP	5.7 ± 0.5	21 ± 4	19 ± 4	9.5
TCPP	6.0 ± 0.3	9.4 ± 1.0	8.5 ± 1.9	9.6

emission rate. However, the sorbed fraction is negligible compared with the total emitted amount (around 2% for the two studied materials). However, although q_s is lower for TBP and TCPP than for TEP, the sorbed phase represents a significant part (about 29 and 65%, respectively) of the total emitted mass (Table 5). Thus, at 23 °C, TEP remains in gas phase whereas TCPP is mainly sorbed on the cell surface. As y_0, q_s is the same in the 60 and 120 mL cells (Table 4) and also contributes to validate its principle of measurement. Thus, the total material emission concentration including both the fractions in the gas phase and on cell surfaces can be determined thanks to the y_0 and q_s values.

Method performance

For GC/MS analysis, the limits of detection (LOD) and the limits of quantification (LOQ) for y_0 and q_s were determined in SIM mode for a signal to noise ratio of 3 and 10, respectively. Results given in Table 6 show that the LOD are comprised of between 1.1 and 2.5 μg/m^3 for y_0 measurement. Obviously, an extraction time longer than 15 min would improve sensitivity but for a screening of OPs indoor sources, these LOD values appear to be sufficient. Increasing the sampler volume improves LOD for q_s. Indeed, for the same surface concentration, the total amount sorbed on the cell inner walls is higher in the 120 mL cell due to higher sorption area (about 1.75 times higher than in the 60 mL cell); the total mass recovered on the Tenax tube is more important and thus better quantified. The average LOD of q_s thus decreases inversely to the volume, from 4.4 to 2.5 μg/m^2.

Reproducibility was evaluated from seven replicates measured with five different glass cells for different days. SPME fiber was the same for all the replicates but Tenax tubes used for q_s measurement were different. A higher variability in replicate measurements is obtained with the 120 mL cell (Tables 2 and 4). Average relative standard deviation (RSD) for y_0 is 24% against only 5% for the 60 mL cell. For q_s it is 15% in 60 mL cell against 20% in 120 mL cell. Another drawback of the high volume sampler is the increase of the equilibrium time which may limit on-site application.

These results should be taken into account for future method improvement to tend towards the best compromise between sensitivity, reproducibility, and sampling time.

Determination of K_{glass}

The cell surface/air partition coefficients K_{glass} were determined according to Eq. 1. Results obtained are shown in Table 7. For each compound studied in the 60 mL cell, K_{glass} values are in the same order level for the two values of y_0 tested (two different materials), confirming the assumption of linear sorption isotherm described in Eq. 1. For a given compound, the observed variation in K_{glass} values for a same material could probably be caused by cumulative experimental errors in y_0 and q_s determination but could also be due to the inhomogeneity of OPs distribution in polyurethane foams.

The cell surface/air partition coefficients of studied OPs range from 1.72×10^{-4} for TEP to 1.68×10^{-2} m for TCPP (average values); as could be expected, K_{glass} decreases with a compound's volatility. These results are consistent with the

Table 5 Distribution of OPs between the gas phase and the sorbed phase. In brackets: percentage of the introduced amount

	60 mL cell				120 mL cell	
	PU + 5% OPs		PU + 7.6% OPs		PU + 7.6% OPs	
	Amount in gas phase (ng)	Amount in sorbed phase (ng)	Amount in gas phase (ng)	Amount in sorbed phase (ng)	Amount in gas phase (ng)	Amount in sorbed phase (ng)
TEP	12367 *(97.8%)*	275 *(2.2%)*	23735 *(98.2%)*	437 *(1.8%)*	41802 *(98.2%)*	765 *(1.8%)*
TBP	91 *(69.5%)*	40 *(30.5%)*	356 *(70.6%)*	148 *(29.4%)*	634 *(73.5%)*	228 *(26.5%)*
TCPP	17 *(28.8%)*	42 *(71.2%)*	39 *(37.1%)*	66 *(62.9%)*	72 *(40.7%)*	105 *(60.3%)*

Table 6 Limits of detection (LOD), limits of quantification (LOQ), and reproducibility (RSD) obtained for GC-MS analysis, in a 60 mL cell, at 23 °C. SPME time = 15 min

	y_0			q_s		
	LOD (μg/m^3)	LOQ (μg/m^3)	RSD (%)	LOD (μg/m^2)	LOQ (μg/m^2)	RSD (%)
TEP	2.5	7.6	2.5	2.1	6.3	22.4
TBP	1.2	3.7	3.9	8.2	24.9	13.9
TCPP	1.1	3.5	9.8	2.8	8.5	7.8

literature. A linear relationship between the logarithm of vapor pressure (V_p) and the logarithm of the stainless steel/air partition coefficient (K_{ss}) was already shown for SVOCs (phthalates) [38]. For the OPs studied, a linear relationship was also found between log K_{glass} and log V_p (Fig. 4a). This would permit determining K_{glass} for different SVOCs when V_p is known, and thus predicting the partition between the gas phase and the sorbed phase on glass.

In this study, K_{glass} could not be experimentally determined for five OPs, as these compounds were neither detected in gas phase nor in sorbed phase. Therefore, their K_{glass} were estimated from the linear relationship of Fig. 4a together with those of 10 others SVOCs: di(2-ethylhexyl)phthalate (DEHP), benzyl butyl phthalate (BBP), di-n-butyl phthalate (DnBP), di-isobutyl phthalate (DiBP), di-isononyl phthalate (DiNP), Phenol, *N*-methyl perfluorooctane sulfonamidoethanol (NMeFOSE), 2,2′,4,4′-tetrabromodiphenyl ether (BDE-47), 2,2′,4,4′,5-pentabromodiphenyl ether (BDE-99), and Bisphenol A (BPA). In the same way, the sorption stainless steel/air partition coefficient (K_{ss}) was estimated for the studied OPs from literature data (Table 8).

These K_{glass} values are the first data available for estimation of SVOCs partition between glass surfaces indoors (e.g., windows) and air. These can be useful for estimation of sink effects and indoor air quality modeling.

As K_{glass} and K_{ss} depend on the vapor pressure, a linear relationship between log K_{glass} and log K_{ss} logically exists (Fig. 4b).Thus, knowing one of the coefficients, the other can be estimated. K_{ss} being 30-8000 times higher than K_{glass}, SVOCs sorption on stainless steel seems to be much more favored than on glass. In the particular case of the presented studies, the choice of glass rather than stainless steel as material of the emission cell was thus judicious: the gas phase is favored in the partition and the sensitivity is thus greater for y_0 measurement. Of course, measurements or estimations performed on specifically treated surfaces (electropolished stainless steel, silanized glass…) could lead to a different material rating.

Figure 4c shows that a relationship between log K_{glass} and log K_{oa} also exists but the octanol/air partition coefficient seems to be a poorer indicator of the cell surface/air partition than the vapor pressure. This suggests that the observed sink effects are rather condensation phenomena than adsorption.

K_{glass} estimation for SVOCs allows the prediction of the behavior of these compounds in the developed sampler. According to the obtained results, the developed emission cell would be adapted to y_0 measurement of DnBP or NMeFOSE. K_{glass} value of DnBP (2.26×10^{-2} m) is very close to that of TCPP (1.68×10^{-2} m). Therefore, partition within the cell would be quite close to that of TCPP, with a gas part of about 30% of the total emitted mass. In the same way, estimated K_{glass} value of NMeFOSE (6.79×10^{-3} m) is between those of TBP (3.37×10^{-3} m) and TCPP (1.68×10^{-2} m). Furthermore, as for TCPP and TBP, its sorbed phase recovery rate would be less than 60% with the implemented method.

Table 7 Calculated values of K_{glass} at 23 °C (m), based on Eq. 1. Standard deviations are calculated from five replicates

	60 mL cell		120 mL cell
	PU + 5% OPs	PU + 7.6% OPs	PU + 7.6% OPs
TEP	$(1.84 \pm 0.45) \times 10^{-4}$	$(1.47 \pm 0.38) \times 10^{-4}$	$(1.84 \pm 0.42) \times 10^{-4}$
TBP	$(3.51 \pm 0.51) \times 10^{-3}$	$(2.98 \pm 0.80) \times 10^{-3}$	$(3.61 \pm 0.76) \times 10^{-3}$
TCPP	$(2.21 \pm 0.15) \times 10^{-2}$	$(1.37 \pm 0.22) \times 10^{-2}$	$(1.47 \pm 0.23) \times 10^{-2}$

Conclusion

A sampler and a method were developed for the determination of the gas-phase concentration of SVOCs at the material surface (y_0), which is often a missing data in the works dealing with exposure assessment and indoor air quality modeling. Compared with the existing methods, which mostly measure emission rates, the approach of experimentally measuring y_0 is original and is the first allowing on-site sampling for realistic emission source assessment. The geometry of the sampler was studied and dimensions were optimized to reduce the sink effects and the sampling time. The device also permits the evaluation of the SVOCs fraction deposited on the glass walls of the cell (q_s), which can represent a significant part of the total emitted amount. Measuring the deposited fraction allows to understand the SVOCs sorption phenomena within the cell and to document the cell surface/air partition coefficients (K_{glass}), which are the first data available for estimation of SVOCs partitions between glass surfaces indoors (e.g., windows) and air.

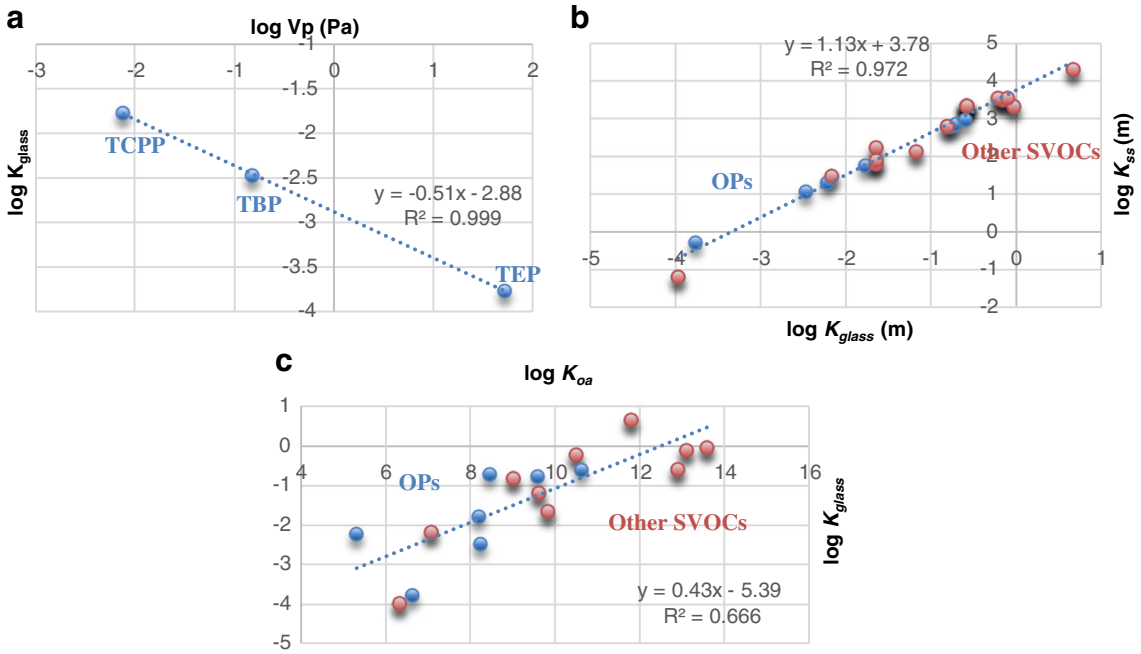

Fig. 4 Relationships between: log K_{glass} and log V_p (**a**), log K_{ss} and log K_{glass} (**b**), and log K_{glass} and log K_{oa} (**c**)

Table 8 Values of the cell surface/air partition coefficient (K_{glass}) for SVOCs compared with stainless steel surface/air partition coefficient (K_{ss})

	K_{glass} (m) (from this study)		K_{ss} (m) (from literature)		
	Measured (average values)	Estimated	Measured values from Liang et al. [38]	Estimated values from Liang et al. [38]	Values reported by Wu et al. [37]
TEP	1.72×10^{-4}			5.23×10^{-1}	
TBP	3.37×10^{-3}			1.16×10^{1}	
TCEP		6.04×10^{-3}		2.01×10^{1}	
TCPP	1.68×10^{-2}			5.65×10^{1}	
TCP		1.72×10^{-1}		6.33×10^{2}	
TPP		1.94×10^{-1}		7.19×10^{2}	
TDCPP		2.52×10^{-1}		9.38×10^{2}	
DEHP		2.62×10^{-1}	2.20×10^{3}		
DEHP		2.62×10^{-1}			1.70×10^{3}
DEHP		2.62×10^{-1}			1.90×10^{3}
DEHP		2.62×10^{-1}			1.50×10^{3}
DEHP		2.62×10^{-1}			1.50×10^{3}
BBP		1.54×10^{-1}	6.20×10^{2}		
DnBP		2.26×10^{-2}	6.30×10^{1}		
DnBP		2.26×10^{-2}			1.74×10^{2}
DnBP		2.26×10^{-2}			8.00×10^{1}
DiBP		6.65×10^{-2}			1.35×10^{2}
DiNP		9.32×10^{-1}	2.10×10^{3}		
Phenol		1.07×10^{-4}			6.50×10^{-2}
NMeFOSE		6.79×10^{-3}			3.00×10^{1}
BDE-47		6.07×10^{-1}			3.50×10^{3}
BPA		7.87×10^{-1}			3.50×10^{3}
BDE-99		4.63×10^{0}			2.00×10^{4}

Acknowledgements The authors acknowledge ADEME (French Agency of Environment and Energy Mastery) for financial support (PhD agreement ADEME TEZ13-03).

Compliance with ethical standards

Conflict of interest The authors declare that they have no conflicts of interest.

References

1. Hartmann PC, Bürgi D, Giger W. Organophosphate flame retardants and plasticizers in indoor air. Chemosphere. 2004;57:781–7.
2. Weschler CJ, Nazaroff WW. Semivolatile organic compounds in indoor environments. Atmos Environ. 2008;42:9018–40.
3. Marklund A, Andersson B, Haglund P. Organophosphorus flame retardants and plasticizers in air from various indoor environments. J Environ Monit. 2005;7:814–9.
4. Reemtsma T, Quintana JB, Rodil R, García-López M, Rodríguez I. Organophosphorus flame retardants and plasticizers in water and air. I. Occurrence and fate. TrAC Trends Anal Chem. 2008;27:727–37.
5. Saito I, Onuki A, Seto H. Indoor organophosphate and polybrominated flame retardants in Tokyo. Indoor Air. 2007;17:28–36.
6. Langer S, Fredricsson M, Weschler CJ, Bekö G, Strandberg B, Remberger M, et al. Organophosphate esters in dust samples collected from Danish homes and daycare centers. Chemosphere. 2016;154:559–66.
7. Cristale J, Hurtado A, Gómez-Canela C, Lacorte S. Occurrence and sources of brominated and organophosphorus flame retardants in dust from different indoor environments in Barcelona, Spain. Environ Res. 2016;149:66–76.
8. Stapleton HM, Klosterhaus S, Eagle S, Fuh J, Meeker JD, Blum A, et al. Detection of organophosphate flame retardants in furniture foam and U.S. house dust. Environ Sci Technol. 2009;43:7490–5.
9. Luongo G, Östman C. Organophosphate and phthalate esters in settled dust from apartment buildings in Stockholm. Indoor Air. 2015. doi:10.1111/ina.12217.
10. Clausen PA, Hansen V, Gunnarsen L, Afshari A, Wolkoff P. Emission of di-2-ethylhexyl phthalate from PVC flooring into air and uptake in dust: emission and sorption experiments in FLEC and CLIMPAQ. Environ Sci Technol. 2004;38:2531–7.
11. Staaf T, Ostman C. Organophosphate triesters in indoor environments. J Environ Monit. 2005;7:883–7.
12. Wensing M, Uhde E, Salthammer T. Plastics additives in the indoor environment–flame retardants and plasticizers. Sci Total Environ. 2005;339:19–40.
13. Weschler CJ, Nazaroff WW. SVOC partitioning between the gas phase and settled dust indoors. Atmos Environ. 2010;44:3609–20.
14. Salthammer T, Bahadir M. Occurrence, dynamics, and reactions of organic pollutants in the indoor environment. CLEAN Soil Air Water. 2009;37:417–35.
15. Beth-Hubner M, Devilliers B. Toxicological evaluation and classification of the genotoxic, carcinotoxic, reprotoxic, and sensitising potential of the tris(2-chloroethyl)phosphate. Int Arch Occup Environ Health. 1999;72:17–23.
16. Doull J, Cattley R, Elcombe C, Lake BG, Swenberg J, Wilkinson C, et al. A cancer risk assessment of di(2-ethylhexyl)phthalate: application of the new U.S. EPA Risk Assessment Guidelines. Regul Toxicol Pharmacol. 1999;29:327–57.
17. Willhite CC. Weight-of-evidence versus strength-of-evidence in toxicologic hazard identification: di(2-ethylhexyl)phthalate (DEHP). Toxicology. 2001;160:219–26.
18. World Health Organization (1990) Tricresyl phosphate. Environ Health Criteria 110
19. Heudorf U, Mersch-Sundermann V, Angerer J. Phthalates: toxicology and exposure. Int J Hyg Environ Health. 2007;210:623–34.
20. Ezechiáš M, Svobodová K, Cajthaml T. Hormonal activities of new brominated flame retardants. Chemosphere. 2012;87:820–4.
21. Bourdin D, Mocho P, Desauziers V, Plaisance H. Formaldehyde emission behavior of building materials: on-site measurements and modeling approach to predict indoor air pollution. J Hazard Mater. 2014;280:164–73.
22. Little JC, Weschler CJ, Nazaroff WW, Liu Z, Cohen Hubal EA. Rapid methods to estimate potential exposure to semivolatile organic compounds in the indoor environment. Environ Sci Technol. 2012;46:11171–8.
23. Kemmlein S, Hahn O, Jann O. Emissions of organophosphate and brominated flame retardants from selected consumer products and building materials. Atmos Environ. 2003;37:5485–93.
24. Salthammer T, Fuhrmann F, Uhde E. Flame retardants in the indoor environment – Part II: release of VOCs (triethylphosphate and halogenated degradation products) from polyurethane. Indoor Air. 2003;13:49–52.
25. Rauert C, Lazarov B, Harrad S, Covaci A, Stranger M. A review of chamber experiments for determining specific emission rates and investigating migration pathways of flame retardants. Atmos Environ. 2014;82:44–55.
26. Clausen PA, Liu Z, Kofoed-Sorensen V, Little J, Wolkoff P. Influence of temperature on the emission of di-(2-ethylhexyl)phthalate (DEHP) from PVC flooring in the emission cell FLEC. Environ Sci Technol. 2012;46:909–15.
27. Jeon S, Kim KT, Choi K. Migration of DEHP and DINP into dust from PVC flooring products at different surface temperature. Sci Total Environ. 2016;547:441–6.
28. Lyng NL, Gunnarsen L, Andersen HV, Kofoed-Sørensen V, Clausen PA. Measurement of PCB emissions from building surfaces using a novel portable emission test cell. Build Environ. 2016;101:77–84.
29. Katsumata H, Murakami S, Kato S, Hoshino K, Ataka Y. Measurement of semivolatile organic compounds emitted from various types of indoor materials by thermal desorption test chamber method. Build Environ. 2008;43:378–83.
30. ISO 16000-25 (2011) Indoor air – Part 25: determination of the emission of semivolatile organic compounds by building products – micro-chamber method. Int Organ Stand
31. Xu Y, Liu Z, Park J, Clausen PA, Benning JL, Little JC. Measuring and predicting the emission rate of phthalate plasticizer from vinyl flooring in a specially-designed chamber. Environ Sci Technol. 2012;46:12534–41.
32. Wu Y, Cox SS, Xu Y, Liang Y, Won D, Liu X, et al. A reference method for measuring emissions of SVOCs in small chambers. Build Environ. 2016;95:126–32.
33. Liang Y, Xu Y. The influence of surface sorption and air flow rate on phthalate emissions from vinyl flooring: measurement and modeling. Atmos Environ. 2015;103:147–55.
34. Cao J, Zhang X, Little JC, Zhang Y (2016) A SPME-based method for rapidly and accurately measuring the characteristic parameter for DEHP emitted from PVC floorings. Indoor Air
35. Nicolle J, Desauziers V, Mocho P, Ramalho O. Optimization of FLEC®-SPME for field passive sampling of VOCs emitted from solid building materials. Talanta. 2009;80:730–7.
36. Desauziers V, Bourdin D, Mocho P, Plaisance H. Innovative tools and modeling methodology for impact prediction and assessment of the contribution of materials on indoor air quality. Herit Sci. 2015;3:28.
37. Wu Y, Xie M, Cox SS, Marr LC, Little JC. A simple method to measure the gas-phase SVOC concentration adjacent to a material surface. Indoor Air. 2015. doi:10.1111/ina.12270.

38. Liang Y, Xu Y. Improved method for measuring and characterizing phthalate emissions from building materials and its application to exposure assessment. Environ Sci Technol. 2014;48:4475–84. doi:10.1021/es405809r.
39. Liu Z, Ye W, Little JC. Predicting emissions of volatile and semivolatile organic compounds from building materials: a review. Build Environ. 2013;64:7–25.
40. Van der Veen I, de Boer J. Phosphorus flame retardants: properties, production, environmental occurrence, toxicity, and analysis. Chemosphere. 2012;88:1119–53.
41. Horrocks AR, Davies PJ, Kandola BK, Alderson A. The potential for volatile phosphorus-containing flame retardants in textile backcoatings. J Fire Sci. 2007;25:523–40.
42. Dishaw LV, Powers CM, Ryde IT, Roberts SC, Seidler FJ, Slotkin TA, et al. Is the PentaBDE replacement, tris(1,3-dichloro-2-propyl) phosphate (TDCPP), a developmental neurotoxicant? Studies in PC12 cells. Toxicol Appl Pharmacol. 2011;256:281–9.
43. Ni Y, Kumagai K, Yanagisawa Y. Measuring emissions of organophosphate flame retardants using a passive flux sampler. Atmos Environ. 2007;41:3235–40.
44. Ali N, Dirtu AC, Van den Eede N, Goosey E, Harrad S, Neels H, et al. Occurrence of alternative flame retardants in indoor dust from New Zealand: indoor sources and human exposure assessment. Chemosphere. 2012;88:1276–82.
45. US Environmental Protection Agency's Office of Pollution Prevention and Toxics, Syracuse Research Corporation (2012) EPI suiteTM
46. Ghislain M, Beigbeder J, Dumazert L, Lopez-Cuesta J-M, Lounis M, Leconte S, et al. Determination of the volatile fraction of phosphorus flame retardants in cushioning foam of upholstered furniture: towards respiratory exposure assessment. Environ Monit Assess. 2016;188:576.
47. ISO 16000-11 (2006) Indoor air – Part 11: Determination of the emission of volatile organic compounds from building products and furnishing – sampling, storage of samples and preparation of test specimens. Int Organ Stand
48. Isetun S, Nilsson U, Colmsjö A, Johansson R. Air sampling of organophosphate triesters using SPME under non-equilibrium conditions. Anal Bioanal Chem. 2004;378:1847–53.
49. Isetun S, Nilsson U, Colmsjö A. Evaluation of solid-phase microextraction with PDMS for air sampling of gaseous organophosphate flame-retardants and plasticizers. Anal Bioanal Chem. 2004;380:319–24.
50. Isetun S, Nilsson U. Dynamic field sampling of airborne organophosphate triesters using solid-phase microextraction under equilibrium and non-equilibrium conditions. Analyst. 2005;130:94–138.
51. Ellis J, Shah M, Kubachka KM, Caruso JA. Determination of organophosphorus fire retardants and plasticizers in wastewater samples using MAE-SPME with GC-ICPMS and GC-TOFMS detection. J Environ Monit. 2007;9:1329–36.
52. Aragón M, Borrull F, Marcé RM. Thermal desorption-gas chromatography-mass spectrometry method to determine phthalate and organophosphate esters from air samples. J Chromatogr A. 2013;1303:76–82.